Discrete wavelet transform application in a CNN-based reverse time migration with multiple energy

Shang Huang and Daniel Trad
shang.huang1@ucalgary.ca

Abstract

In seismic imaging, image resolution and accuracy are affected by migration approaches. Deep learning has recently been considered an alternative and efficient way to improve image quality. In this project, discrete wavelet transform (DWT) is applied with U-Net on migration data containing multiple energy. The neural network approximates the inverse of the Hessian to obtain high-quality reflectivity prediction. Results show that the DWT subband helps the model learn smooth input, extract critical features from data, and enhance image resolution. Multiple energy provides valuable information for subsurface structure expanding prediction illumination.

Theory

DWT in two dimensions

Based on Acharya and Ray (2005), the two-dimensional scaling functions can be expressed as separable functions, which are the product of two one-dimensional scaling functions. If an image has M rows and N columns, applying the one-dimensional transform in each row, two subbands are produced in each row with a size of M x $\frac{N}{2}$. Then applying a one-dimensional DWT column-wise on the subbands (intermediate result), four subbands LL, LH, HL, and HH are obtained with the size of $\frac{M}{2}$ x $\frac{N}{2}$, respectively. LH, HL and HH contain the high-frequency information around discontinuities (edges in an image) in the input signal. LL is a coarser version of the original input signal and provides an input to the next decomposition level.

$$\text{LL wavelet: } \psi^1(m,n) = \phi(m)\psi(n) \quad (1)$$

$$\text{HL wavelet: } \psi^2(m,n) = \psi(m)\phi(n) \quad (2)$$

$$\text{HH wavelet: } \psi^3(m,n) = \psi(m)\psi(n) \quad (3)$$

$$\text{Approximation LL: } \phi^2(m,n) = \phi(m)\phi(n) \quad (4)$$

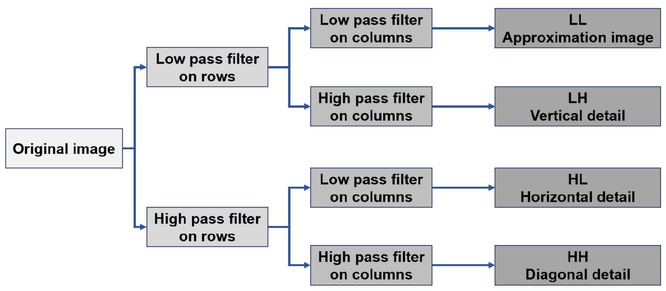

FIG. 1: Block diagram of DWT.

Neural network training strategy

In this project, we propose to use U-Net (Ronneberger et al., 2015) with additional skip connection layers to learn patterns from migrated images and discrete wavelet transform filtered images. Figure 2 illustrates the DWT applied U-Net architecture. The network operator acts as an approximation of the inverse of the Hessian (Kaur et al., 2020; Torres and Sacchi, 2022), to filter migrated data into a predicted reflectivity model, but with more physical data constraints in the input channel.

$$\mathbf{m}_{pred} = \Gamma_{unet}(\mathbf{m}_{rtmm}, \mathbf{m}_{refl}, \mathbf{m}_{rtmm_{DWT}}) \quad (5)$$

where $\mathbf{m}_{rtmm}$ is the RTMM initial image, $\mathbf{m}_{refl}$ denotes the smooth background reflectivity model, $\mathbf{m}_{rtmm_{DWT}}$ means DWT subband on RTMM image, and $\mathbf{m}_{pred}$ represents the output reflectivity coefficient prediction.

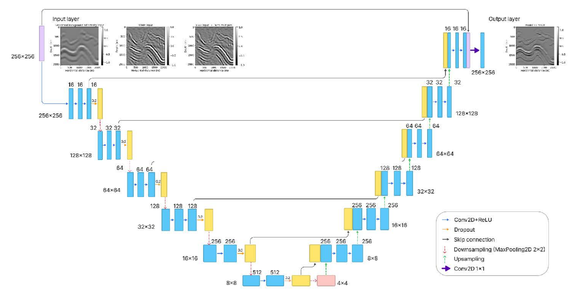

FIG. 2 Architecture of DWT applied in the RTMM-CNN.

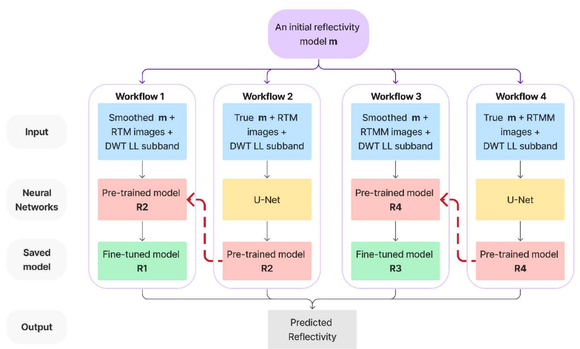

FIG. 3: Neural network model plan and workflows.

Train and test set

We have used Sigsbee2b, Amoco, Agbami, Pluto, BP2004 and Marmousi and our defined model as the original input set. Eight meters is used as the spatial interval for each grid point. The total record time is 7.2 seconds with 0.8 of milliseconds temporal sampling. The shot and receiver intervals are 80 and 16 meters, respectively. A fourth-order finite different method is used for the forward modeling. Model R1 is chosen as our baseline model without using multiple energy. The approximation image is the third channel input. Before training, the whole RTM and RTMM images, and the LL subband were partly chosen and divided randomly into 1900 different spatial windows with 256x256 points. The train and test set ratio is 0.8: 0.2. All the output predictions have normalized scaling.

Numerical examples

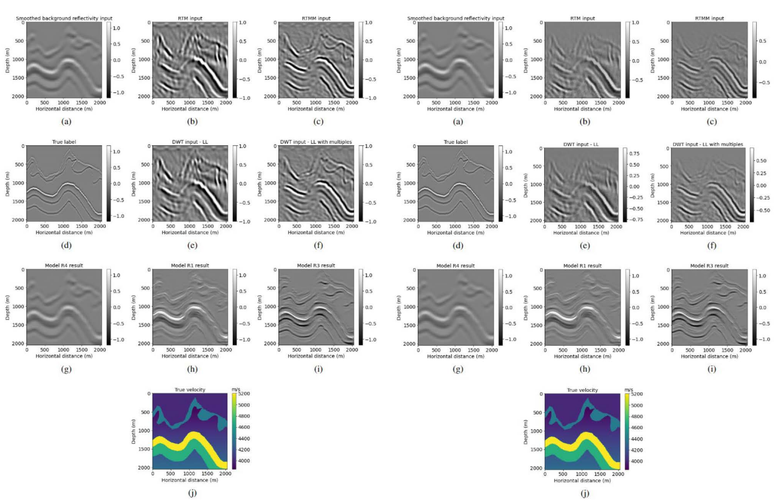

FIG. 4: Windowed Foothills example. FIG. 5: Windowed Foothills example with noise.

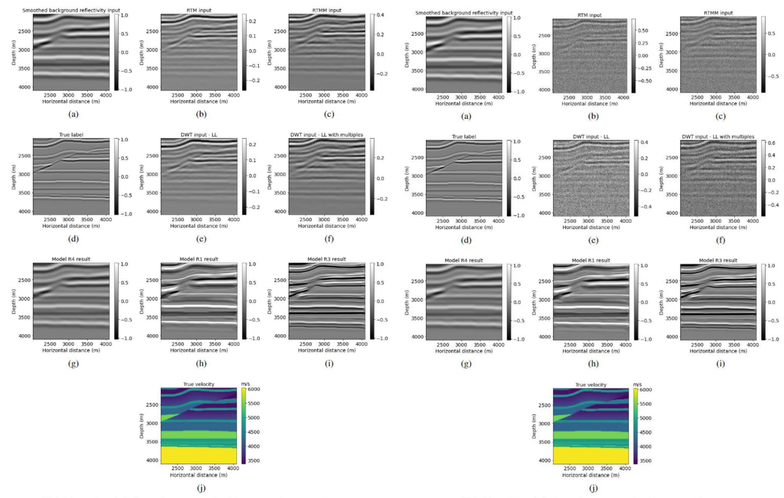

FIG. 6: Windowed Overthrust example.

FIG. 7: Windowed Overthrust example with noise.

The proposed technique has been tested on the Foothills and Overthrust geology models respectively. When windowing the inputs, to obtain a subband LL image with the same size as input migration images, we applied a bicubic interpolation with factor 2 on the LL image. Model R3 results, which contains multiple energy, have improved resolution and accurate reflector prediction than baseline model R1 or pre-conditioned model R4.

Conclusion

RTMM-CNN with a DWT subband channel can provide improved reflectivity coefficient prediction. DWT subband LL and pre-trained model let the fine-tuned model learn to extract key features from low-frequency information and tolerate more artifacts from smooth input. Multiple energy is a supplement tool providing additional subsurface illumination, and helping neural network distinguish signals from noise. The neural network operator acts as an approximation of the inverse of the Hessian, which can suppress image artifacts and improve the reflectivity resolution. The next step is to let the model learn how to predict a geology model with rapid lateral velocity change and test it in the field data.

Acknowledgement

We thank the sponsors of CREWES for continued support. This work was funded by CREWES industrial sponsors and NSERC (Natural Science and Engineering Research Council of Canada) through the grant CRDPJ 543578-19. The first author was partially supported by a scholarship from the China Scholarship Council (CSC).

References

Acharya, T., and Ray, A. K., 2005, Image processing: principles and applications, Chapter 5: John Wiley & Sons.

Ronneberger, O., Fischer, P., and Brox, T., 2015, U-net: Convolutional networks for biomedical image segmentation, in International Conference on Medical image computing and computer-assisted intervention, Springer, 234–241.

Kaur, H., Pham, N., and Fomel, S., 2020, Improving the resolution of migrated images by approximating the inverse hessian using deep learning: Geophysics, 85, No. 4, WA173–WA183.

Torres, K., and Sacchi, M., 2022, Least-squares reverse time migration via deep learning-based updating operators: Geophysics, 87, No. 6, 1–80

NSERC CRSNG
UNIVERSITY OF CALGARY
FACULTY OF SCIENCE
Department of Geoscience